Time-varying MHD flows with free surfaces

John Mooney, Nick Stokes

CSIRO Division of Mathematical and Information Sciences, Clayton, Victoria.

ABSTRACT

The numerical requirements for MHD flows with free surfaces are considerable. A stable, time-accurate Navier-Stokes solver is needed, with the ability not only to handle free surfaces in the presence of strong internal circulations, but also to allow for surface tension, while still controlling surface instabilities. Another requirement is the flexibility to handle the electromagnetic fields, which will normally have to be solved inside and outside the fluid domain. Finally, there is the issue of turbulence, complicated by the anisotropy of the force field.

To do this with any efficiency requires substantial segregation of the variables in the algorithm. This paper describes an approach using operator splitting and conjugate gradient methods, and developed with the partial differential equations solving program *Fastflo*.

1. NOMENCLATURE

x, y, z	cartesian coordinates
t	time
L_x	x-length of tank (North-South)
L_y	y-length of tank (East-West)
H	height of tank
H_f	initial height of liquid metal
Ω_1	liquid metal region
Ω_2	air space above liquid metal
Ω	full computational domain ($\Omega_1 \cup \Omega_2$)
Γ_f	free surface of liquid metal ($\Omega_1 \cap \Omega_2$)
$\mathbf{n}$	unit normal to Γ_f
z_f	height of free surface
ρ	density of liquid metal
η	dynamic viscosity
ν	kinematic viscosity (η/ρ)
σ	electrical conductivity
μ	magnetic permeability of free space
$\mathbf{u}$	liquid metal velocity
p	pressure
$\mathbf{f}$	body force per unit volume
$\mathbf{g}$	gravitational acceleration
$\dot{\mathbf{X}}$	mesh deformation velocity
$\mathbf{B}$	magnetic field (magnetic induction)
$\mathbf{E}$	electric field
$\mathbf{j}$	electric current density
ϕ	scalar electrodynamic potential
$\mathbf{A}$	vector electrodynamic potential
$\mathbf{F}_L$	Lorentz force per unit volume
Rm	magnetic Reynolds number

SI units are used throughout.

2. Overview of problem and methods

The flow of molten metals subject to electromagnetic fields involves solving the Navier-Stokes equations for the liquid and the Maxwell equations to determine the body forces. These effects are coupled. In addition, in industrial problems there are often free surfaces which are affected by the electromagnetic fields. The boundary conditions here are complicated by the fact that those fields extend into the space beyond.

Where complicated geometries are involved, it is desirable to use an unstructured mesh for solving the equations, and the finite element method is attractive. Because of the complexity of the interacting effects, we used the finite element package *Fastflo*, which allows a number of interactive problems to be specified in a high level language, and can incorporate the free surface effects as well as the electromagnetics.

3. The test problem

The test problem was posed by BHP Research, as part of the joint *Fastflo* project. A rectangular tank is filled with a liquid metal, with a magnetic field applied from two

box-shaped poles adjacent to the East and West walls, with a potential difference applied across the North and South walls. Simulations were carried out for a steady applied potential difference and an alternating potential difference (1 Hz).

4. The Navier-Stokes equations

The Navier-Stokes equations are set up in a suitable weak form. In the problem to be described here the surface tension is negligible, and the appropriate natural boundary condition is one of zero stress. This applies at the free surface, where it is also convenient to take the pressure as zero. On the walls and bottom a no slip condition is used (and appropriate symmetry conditions on the symmetry planes $x, y = 0$).

To present the momentum equations in the appropriate weak form we define the function spaces:

$$\mathcal{V}_0 = \{\mathbf{v} | \mathbf{v} \in H^1(\Omega_1), \quad \mathbf{v} = \mathbf{0} \quad \text{on} \quad \partial\Omega_1\},$$

$$\mathcal{H} \;=\; L^2(\Omega_1).$$

Here $\partial\Omega_1$ represents the total no slip boundary (walls and bottom). The momentum equation and continuity constraint in weak form are

$\forall \mathbf{v} \in \mathcal{V}_0, \quad \forall q \in \mathcal{H},$

$$\int_{\Omega_1} \rho \frac{\partial \mathbf{u}}{\partial t} \cdot \mathbf{v} \, dx + \mathcal{P}(\mathbf{u}, \mathbf{v}) - \int_{\Omega_1} p \, \nabla \cdot \mathbf{v} \, dx = \int_{\Omega_1} \mathbf{f} \cdot \mathbf{v} \, dx, \tag{1}$$

$$\int_{\Omega_1} \nabla \cdot \mathbf{u} \, q \, dx = 0, \tag{2}$$

$$\text{where } \mathcal{P}(\mathbf{u}, \mathbf{v}) = \int_{\Omega_1} \eta \nabla \mathbf{u} \cdot \nabla \mathbf{v} \, dx + \int_{\Omega_1} \eta \sum_{i=1}^{3} \frac{\partial \mathbf{u}}{\partial x_i} \cdot \nabla v_i \, dx + \int_{\Omega_1} \rho \left([\mathbf{u} + \dot{\mathbf{X}}] \cdot \nabla\right) \mathbf{u} \cdot \mathbf{v} \, dx. \tag{3}$$

Here $\mathbf{v}$ denotes a vector test function, and q is scalar test function. We seek a solution $\mathbf{u} \in \mathcal{V}_0$ and $p \in \mathcal{H}$. In practice the solutions are sought in suitable finite dimensional spaces; typically using quadratic finite elements for velocity and linear for pressure. The $\dot{\mathbf{X}}$ term in the momentum equation (3) represents the effect of mesh motion.

On the free surface Γ_f, in addition to the natural zero stress condition, the flow field must also satisfy the *kinematic condition*

$$u_z = \frac{\partial z_f}{\partial t} + u_x \frac{\partial z_f}{\partial x} + u_y \frac{\partial z_f}{\partial y}, \tag{4}$$

where z_f is the height on Γ_f measured from the bottom of the tank ($z = 0$). The kinematic condition relates the rate of displacement of the free surface to the instantaneous fluid velocity. The zero surface stress and the kinematic condition define a unique flow field and free boundary Γ_f.

The influence of the electromagnetic field on the fluid motion is felt through the Lorentz force, which contributes to the body force in the momentum equation:

$$\mathbf{f} = \rho \mathbf{g} + \mathbf{F}_L = \rho \mathbf{g} + \mathbf{j} \times \mathbf{B}. \tag{5}$$

The changing electromagnetic field caused by the liquid motion is also computed.

Segregated time stepping algorithm

In three dimensions it is only feasible to solve the coupled equations for the flow variables and electromagnetic field variables as well as the free surface motion by some type of segregated solver process. The algorithm used for the electromagnetic free surface problem is outlined here.

An initial flow field, an initial electromagnetic field and an initial liquid free surface are specified. For this problem the liquid starts at rest with a free surface of uniform height ($z = H_f$). The primary electromagnetic field is applied as specified in section 5. For the first step the Lorentz force is computed and a new liquid velocity and pressure is calculated. Then the electromagnetic field is updated according to the new velocity field. Finally, the free surface is adjusted in accordance with the kinematic condition and the mesh distorted above and below the surface to achieve this motion. This process is repeated for subsequent steps. The algorithm generates a sequence of velocity/pressure fields $\{\mathbf{u}^n, p^n\}$, a sequence of electromagnetic fields $\{\mathbf{B}^n, \mathbf{E}^n\}$ [or $\{\mathbf{A}^n, \phi^n\}$ in the A-ϕ formulation] and a corresponding sequence of meshes

$\{\Omega_1^n\}$, $\{\Omega_2^n\}$ approximating the flow region and the air space.

Algorithm: $\{\mathbf{u}^n, p^n, \mathbf{B}^n, \mathbf{E}^n, \Omega_1^n, \Omega_2^n\} \rightarrow \{\mathbf{u}^{n+1}, p^{n+1}, \mathbf{B}^{n+1}, \mathbf{E}_1^{n+1}, \Omega_1^{n+1}, \Omega_2^{n+1}\}$:

Step 1. Solve flow equations for $\mathbf{u}^{n+1}$, p^{n+1}: $\forall \mathbf{v} \in \mathcal{V}_0,\ \forall q \in L^2(\Omega_1^n)$,

$$\int_{\Omega_1^n} \frac{\mathbf{u}^{n+1} - \mathbf{u}^n}{\Delta t} \cdot \mathbf{v}\, dx + \mathcal{P}(\mathbf{u}^{n+1}, \mathbf{v}) - \int_{\Omega_1^n} p^{n+1}\, \nabla \cdot \mathbf{v}\, dx = \int_{\Omega_1} \mathbf{f} \cdot \mathbf{v}\, dx, \quad (6)$$

$$\int_{\Omega_1^n} \nabla \cdot \mathbf{u}^{n+1}\, q\, dx = 0. \quad (7)$$

This is solved using a conjugate gradient algorithm. To do this $\mathbf{u}^{n+1}$ is replaced by $\mathbf{u}^n$ in every term in $\mathcal{P}(\mathbf{u}^{n+1}, \mathbf{v})$ (3) except the first (Laplacian).

Step 2. Advance the electromagnetic field: $\mathbf{B}^n, \mathbf{E}^n \rightarrow \mathbf{B}^{n+1}, \mathbf{E}^{n+1}$.

Step 3. Solve for a vertical displacement function $\delta z(x, y)$ on the free surface satisfying the differential equation

$$\frac{\delta z}{\Delta t} + \mathbf{u}^{n+1} \nabla z_f - \alpha \nabla^2 \delta z = u_z^{n+1} \text{ on } \Gamma_f^n. \quad (8)$$

$\alpha \nabla^2 \delta z$ is a smoothing term chosen to stabilise the mesh deformation, with parameter α.

Step 4. Interpolate the vertical displacement $\delta z(x, y)$ throughout Ω^n and advance the mesh for Ω_1^n, Ω_2^n to that for Ω_1^{n+1}, Ω_2^{n+1}.

The overall algorithm segregates the updating of the flow variables from the electromagnetic variables and the mesh motion. The algorithm is formally first order accurate in the time step Δt.

5. Turbulence model

As stated earlier, most liquid metal MHD flows will be turbulent due to the very small kinematic viscosity. However, in the presence of a dominant magnetic field the turbulence structure is substantially altered from the normal situation. According to authorities such as Shercliff (1965) the magnetic field damps out vorticity components orthogonal to the field and the turbulence structure tends to collapse to a system of two-dimensional eddies all aligned in the plane orthogonal to the field lines. This is in contrast to the usual tendency of turbulence to be three-dimensional and isotropic. Furthermore, in some situations turbulence may be completely suppressed by the field and the flow laminarised.

There is no generally accepted turbulence model for MHD flows of liquid metal. Special models have been developed for flows in ducts — see references cited by Araseki & Kotake (1982). Sneyd (1993) and Shercliff (1965) argue that the MHD flow may well be better simulated using a zero-equation eddy-viscosity model. The eddy viscosity determines the overall scale of the velocity field.

In certain liquid metal MHD flows it seems that the eddy viscosity is a constant or nearly so throughout the metal. So for this problem we have chosen to use a constant eddy viscosity ($\eta_t + \eta$). The experimental data of Taberlet & Fautrelle (1985) suggests that the effective viscosity of liquid steel in sustained circulating flows may be in the range 10^4 times the molecular viscosity. This is value used here.

6. Advancing the electromagnetic field

In this section the computational process for updating the electromagnetic field at Step 2 of the full free surface-MHD algorithm (section 3) is described. The generally accepted MHD equations are those of fluid flow plus Maxwells' equations:

$$\nabla \times \mathbf{E} = -\frac{\partial \mathbf{B}}{\partial t} \quad \text{(Faraday's law)} \quad (9)$$

$$\nabla \times \mathbf{B} = \mu \mathbf{j} \quad \text{(Ampère's law)} \quad (10)$$

$$\nabla \cdot \mathbf{B} = 0 \quad (11)$$

$$\mathbf{j} = \sigma(\mathbf{E} + \mathbf{u} \times \mathbf{B}) \quad \text{(Ohm's law)} \quad (12)$$

$$\nabla \cdot \mathbf{j} = 0 \quad \text{(current continuity)} \quad (13)$$

The importance of the diffusion of B through the metal relative to its advection with the fluid is signified by the magnetic Reynolds number $\mathrm{Rm} = UL\sigma\mu$, where U is a characteristic liquid velocity and L is a characteristic length. Here $L = L_y = 1.0$ m and velocities may reach 2 m/s or more, giving $\mathrm{Rm} = 2.8$. This means that advection is significant, and the evolution of B in the metal must be modelled. Because of advection on

the free surface, it is also necessary to allow B to evolve in both the liquid and the air space above. The condition $\mathbf{B} = \mathbf{B}_0$ (fixed magnetic field) is imposed on all outer boundaries of the fixed computational domain Ω.

6.1 A-ϕ formulation

The electromagnetic field can be fully specified by means of a vector electrodynamic potential A and a scalar electrodynamic potential ϕ according to

$$\mathbf{B} = \nabla \times \mathbf{A}, \tag{14}$$

$$\mathbf{E} = -\nabla\phi - \frac{\partial \mathbf{A}}{\partial t}. \tag{15}$$

The A-ϕ formulation allows a natural specification of the electromagnetic boundary conditions and the divergence free condition on B is automatically satisfied. The Lorentz force is easily calculated from the A-ϕ fields and the whole scheme is computationally efficient. The only disadvantage is that if B is required, it has to be obtained by numerical differentiation of A.

To specify A uniquely, we use the Coulomb gauge: $\nabla \cdot \mathbf{A} = 0$, and some fixed (Dirichlet) boundary conditions.

6.2 Boundary conditions for potential and current

Boundary conditions for ϕ (using symmetry) are that

$$\phi = 0 \quad \text{at } x = 0,$$

$$\phi = -V_0(t)/2 \quad \text{at } x = L_x/2. \tag{16}$$

The other electromagnetic boundary conditions relate to electric current: there can be no current flow through the insulating side walls and bottom, nor through the metal/air interface. These conditions are

$$\mathbf{j} \cdot \mathbf{n} = 0 \quad \text{on } \Gamma_f,$$

$$y = 0, \quad y = L_y/2, \quad z = 0. \tag{17}$$

6.3 Evolution equation for A

The evolution equation for A can be derived simply by equating the two expressions for $\mu\mathbf{j}$ implied by (10) and (12): this gives

$$\sigma\mu\frac{\partial \mathbf{A}}{\partial t} = \nabla^2\mathbf{A} + \sigma\mu(-\nabla\phi + \mathbf{u} \times (\nabla \times \mathbf{A})) \quad \text{in} \quad \Omega. \tag{18}$$

This equation holds throughout the metal and air space, with the proviso that $\sigma\mu$ and u vanish in the air space. The equation is a diffusion-advection equation for each component of A, but coupled to ϕ. Equation (18) takes this specific form because of the gauge condition: this allows the awkward vector operator $\nabla\times\nabla\times$ to be replaced by the Laplacian.

Equation (18) has an appropriate weak form that is suitable for the finite element method. The quantities σ, u and $\nabla\phi$ are all piecewise continuous, vanishing in the air space: this presents no difficulty. The weak form has a solution for A which is continuous and has continuous first derivatives throughout Ω, including the interface Γ_f. By (14), this is consistent with continuity of B throughout, including the interface, which is required by the physics.

6.4 Equation for ϕ

To determine E the potential ϕ must be calculated in the metal domain. Substituting in the current continuity equation $\nabla \cdot \mathbf{j} = 0$ gives:

$$\nabla\cdot(-\nabla\phi + \mathbf{u}\times(\nabla\times\mathbf{A})) = 0 \quad \text{in} \quad \Omega_1. \tag{19}$$

Dirichlet boundary conditions for ϕ are given at (16). In addition, the current conditions (17) can be imposed as natural boundary conditions using the appropriate weak formulation.

6.5 Algorithm for update of electromagnetic field

Because the A and ϕ equations are coupled the following type of segregated time stepping algorithm can be used, using the proper weak equations for A anf ϕ. An initial state $\mathbf{A}_0$ is required for A.

Find $\mathbf{A}^{n+1} \in \mathcal{V}_g$ such that $\forall \mathbf{v} \in \mathcal{V}_0$

$$\int_\Omega (\sigma\mu\frac{\mathbf{A}^{n+1} - \mathbf{A}^n}{\Delta t} \cdot \mathbf{v} + \nabla\mathbf{A}^{n+1} \cdot \nabla\mathbf{v})\, dx =$$

$$\int_\Omega \sigma\mu(-\nabla\phi^n + \mathbf{u}^{n+1}\times(\nabla\times\mathbf{A}^n) + \dot{\mathbf{X}}\cdot\nabla\mathbf{A}^n)\cdot\mathbf{v}\, dx, \tag{20}$$

recognising that $\sigma\mu = 0$, $\mathbf{u}^{n+1} = \mathbf{0}$ in Ω_2.

Find $\phi^{n+1} \in \mathcal{W}_g$ such that $\forall w \in \mathcal{W}_0$

$$\int_{\Omega_1} (\nabla\phi^{n+1} + \mathbf{u}^{n+1} \times \nabla \times \mathbf{A}^{n+1})) \cdot \nabla w \, dx = 0. \tag{21}$$

Here $\mathcal{V}_g$, $\mathcal{V}_0$, $\mathcal{W}_g$, $\mathcal{W}_0$ are the appropriate function spaces for (X), (Y). The term in $\dot{\mathbf{X}}$ in (20) is due to mesh motion computing $\mathbf{E}$ from $\mathbf{A}$ using (15).

At each step $\mathbf{A}$ is determined over the full domain, but ϕ is determined only over the metal region.

6.6 Initial and boundary conditions for A

The initial state for $\mathbf{A}$ is taken to be a vector $\mathbf{A}_0$ that represents the magnetic field $\mathbf{B}_0$ of the fixed magnets. This field can be given by a reasonably simple analytic form. The fixed field also appears in the boundary conditions for $\mathbf{A}$.

7. Results

Three characteristic simulations are described here for a steady applied potential difference and an alternating potential difference. The fixed magnetic field has a maximum strength of 0.4 T. In all cases the effective dynamic viscosity is taken to be 64 kg m^{-1} s^{-1} — 10^4 times the molecular viscosity. A potential difference of overall magnitude 0.4 volt is applied across the North/South walls.

The tank dimensions were $L_x = 3$ m, $L_y = 0.5$ m; the initial depth of liquid was 0.7 m and the air space was 0.7 m deep. The computational mesh (including the air space) used is based on a regular 24 by 8 by 22 mesh of rectangular 20-node box elements for the x-, y- and z-directions: this mesh covers the quarter symmetry-reduced computational domain. The element thickness is reduced near the walls. The mesh has a total of 19693 nodes and 4224 elements. The mesh is shown in Fig. 2 (left).

The results for the steady potential difference were obtained using a fixed time step of 0.025 s and a surface smoothing parameter of $\alpha = 0.3$ m^{2}s^{-1}. A total run time of 5 seconds was used for both of these simulations, with a total of 200 time steps. The results for the alternating potential difference were obtained using a fixed time step of 0.05 s and $\alpha = 0.1$ m^{2}s^{-1}. A total run time of 10 seconds was used for this simulation, also with a total of 200 steps.

The gauge condition was satisfied, with $|\nabla \cdot \mathbf{A}| < 10^{-5} \times |\mathbf{A}|$ throughout.

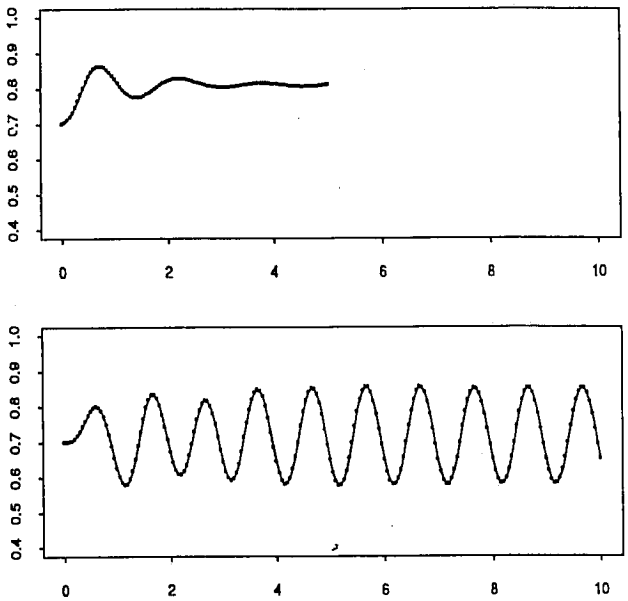

Figure 1 Plots of heights of centre of free surface (at $x, y = 0$) against time for (upper plot) steady potential difference, (lower plot) alternating potential difference. Time is plotted horizontally from 0 to 10 s, height is plotted vertically over range 0.4 to 1.0 m.

Steady potential difference

If the applied potential difference is fixed (constant current case) the system settles to a steady state, at least if the primary Lorentz force is not too strong. As the potential difference is applied two main circulation cells become established, with uplift in the central region and downflow near the ends of the tank. The free surface rises in the central region, then overshoots and decaying oscillations ensue. Fig. 1 (upper) shows through time the height at the centre of the free surface ($x = 0$, $y = 0$). The peak excursion of the surface from the mean level (0.7 m) is 0.11 m. The system seems to have a natural resonant period of about 1.6 s, based on the displayed oscillations of the central height.

The computational meshes at $t = 0$ and $t = 5$ s are shown in Fig. 2. These correspond

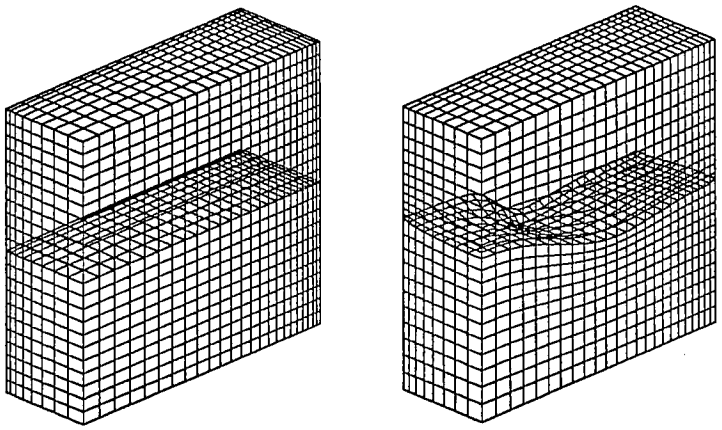

Figure 2 Steady potential difference: computational mesh at $t = 0$ (left) and $t = 5$ s (right). The meshes cover the region $x, y \geq 0$.

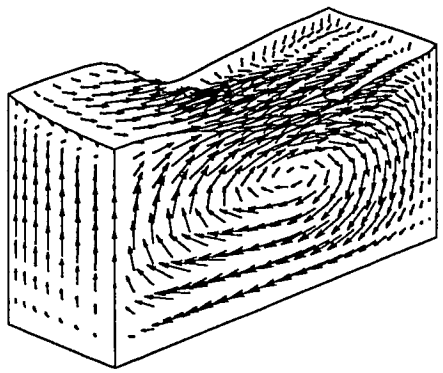

Figure 3 Steady potential difference: velocity field at $t = 5$ s over liquid metal region with $x, y \geq 0$. Peak velocity is 1.416 m/s.

to the symmetry reduced region $x, y \geq 0$. A full view of the whole free surface is shown in grey scale in Fig. 4.

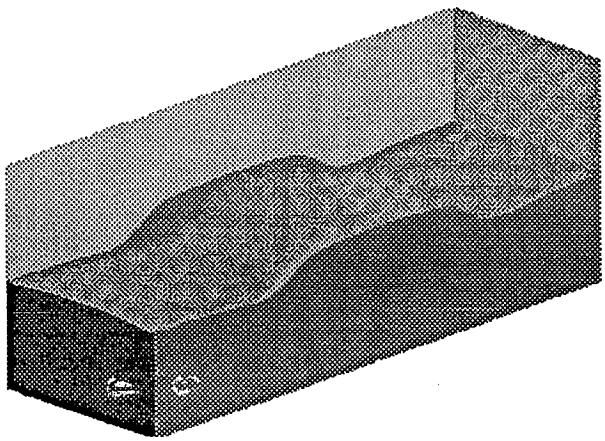

Figure 4 Steady potential difference: complete free surface of liquid metal at $t = 5$ s.

The velocity field at $t = 5$ s over the region $x, y \geq 0$ is plotted with an arrow diagram in Fig. 3 (over the visible surfaces of the metal region). This diagram shows the simple circulation cells at the steady state. The peak velocity is 1.416 m/s.

In the steady state the maximum perturbation to the magnetic field caused by the liquid motion is about 10% in the z-component of $\mathbf{B}$. This is consistent with the intermediate Rm value; the narrow tank and the fixed surface $\mathbf{A}$ and $\mathbf{B}$ also tend to suppress the advective perturbation.

Fig. 5 (left) shows the electric current density vector for the steady state. This is of most interest on the free surface. Clearly, the current is tangential to the surface, as it should be, and is mainly from South to North. However, in the central region there are significant components of current in the orthogonal directions; these are indicated in Fig. 5 (right). These components arise from the $\mathbf{u} \times \mathbf{B}$ part of the current.

Alternating potential difference

The alternating potential difference induces an oscillatory motion of the free surface, with an underlying pair of circulation cells which alternate in flow direction. After a settling time of about 3 s the free surface motion becomes almost perfectly periodic, with period 1 s.

The free surface and velocity arrows at successive quarter periods (0.25 s) are shown over one period (1 s) in Fig. 6, well after the periodic motion has been established ($t \geq 7.60$ s). The difference in the surfaces at $t = 7.85$ and 8.35 s shows that the overall motion of the free surface contains harmonics of the driving frequency $\sin 2\pi t$.

The amplitude of excursion of the free surface from the mean: ~ 0.12 m is similar to the steady case but the peak flow velocities are smaller: 0.773 m/s as compared to 1.416 m/s.

At the low frequency of 1 Hz there is no significant electromagnetic skin effect: in this

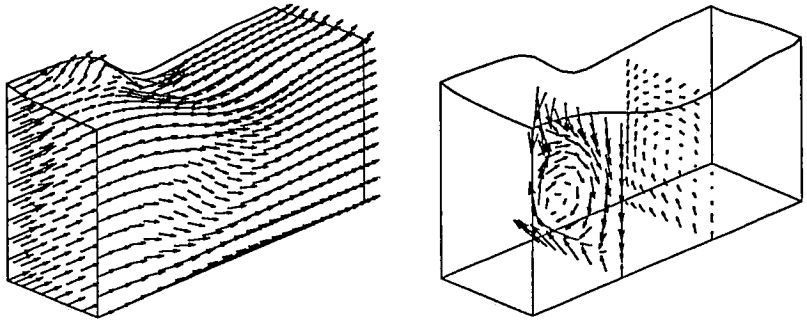

Figure 5 Steady potential difference: electric current density on computational region $x, y \geq 0$ (left) and yz-component of current density on cross sections $x = 0.5, 1$ m (right) at $t = 5$ s. Peak current density is 0.280 A m^{-2}, peak yz-component is 0.229 A m^{-2}.

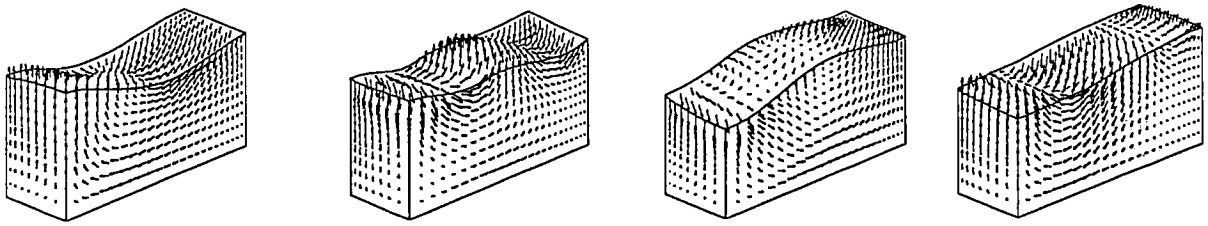

$t = 7.60$ s $t = 7.85$ s $t = 8.10$ s $t = 8.35$ s

Figure 6 Alternating potential difference: velocity fields at successive quarter-period intervals (0.25 s) on computational region $x, y \geq 0$. Peak velocity is 0.773 m/s.

case the skin depth is

$$d \simeq \sqrt{\frac{2}{\mu\sigma}} = 0.47 \text{ m},$$

This is comparable to the fluid depth, so will not have a significant boundary layer effect.

Acknowledgements

This work was sponsored, and the problem specified, by BHP Research as part of the *Fastflo* project. The overall *Fastflo* project received funding under the GIRD scheme, and was managed by a syndicate consisting of BHP, CSIRO and Compumod.

REFERENCES

J. A. Shercliff. 1965, *A Textbook of Magnetohydrodynamics*, Pergmon Press, Oxford.

H. Aresaki & S. Kotake, 1982, " Numerical method for analysis of turbulent liquid metal magnetohydrodynamic flow", *Nucl. Eng. Des.*, **71**, 121–136.

A. D. Sneyd, 1993/4, "Theory of electromagnetic stirring by AC fields", *IMA J. Math. Appl. Business & Industry*, **5**, 87–113 (1993/4).

E. Taberlet & Y. Fautrelle, 1985, "Turbulent stirring in an experimental induction furnace", *J. Fluid Mech.*, **159**, 409–431.